Moulis, J.-M., & Meyer, J. (1982) *Biochemistry 21*, 4762–4771.
Moulis, J.-M., Auric, P., Gaillard, J., & Meyer, J. (1984a) *J. Biol. Chem. 259*, 11396–11402.
Moulis, J.-M., Meyer, J., & Lutz, M. (1984b) *Biochem. J. 219*, 829–832.
Moulis, J.-M., Meyer, J., & Lutz, M. (1984c) *Biochemistry 23*, 6605–6613.
Noodleman, L. (1988) *Inorg. Chem.* (in press).
Noodleman, L., & Baerends, E. J. (1984) *J. Am. Chem. Soc. 106*, 2316–2327.
Noodleman, L., Norman, J. G., Jr., Osborne, J. H., Aizman, A., & Case, D. A. (1985) *J. Am. Chem. Soc. 107*, 3418–3426.
Papaefthymiou, V., Millar, M. M., & Münck, E. (1986) *Inorg. Chem. 25*, 3010–3014.
Sands, R. H. (1979) in *Multiple Electron Resonance Spectroscopy* (Dorio, M. M., & Freed, J. H., Eds.) pp 331–374, Plenum, New York.
Spiro, T. G., Hare, J., Yachandra, V., Gewirth, A., Johnson, M. K., & Remsen, E. (1982) in *Iron-Sulfur Proteins* (Spiro, T. G., Ed.) pp 407–423, Wiley-Interscience, New York.
Sweeney, W. V., & Rabinowitz, J. C. (1980) *Annu. Rev. Biochem. 49*, 139–161.

Effect of Solvent Viscosity on the Heme-Pocket Dynamics of Photolyzed (Carbonmonoxy)hemoglobin†

E. W. Findsen,‡ J. M. Friedman,§ and M. R. Ondrias*,‡

Department of Chemistry, University of New Mexico, Albuquerque, New Mexico 87131, and AT&T Bell Laboratories, Murray Hill, New Jersey 07974

Received March 11, 1988; Revised Manuscript Received July 21, 1988

ABSTRACT: The heme-pocket dynamics subsequent to carbon monoxide photolysis from human hemoglobin have been monitored as a function of glycerol–water solvent composition with time-resolved resonance Raman spectroscopy. Prompt (geminate) ligand recombination rates and the transient heme-pocket geometry established within 10 ns after photolysis appear to be largely independent of solvent composition. The rate of relaxation of the transient geometry to an equilibrium deoxy configuration is, however, quite sensitive to solvent composition. These observations suggest that the former processes result from local, internal motions of the protein, while the relaxation dynamics of the proximal heme pocket are predicated upon more global protein motions that are dependent upon solvent viscosity.

During the past 2 decades, an increasing number of experimental and theoretical studies [for review, see Gurd and Rothgeb (1979), Debrunner and Frauenfelder (1982), Karplus and McCammon (1983), and Rousseau and Friedman (1988)] have demonstrated that structural dynamics play a pivotal role in the functional processes of metalloproteins. The complexity of proteins allows for many levels of structural dynamics, each having the potential to influence net protein function. These can range from local fluctuations of atoms or side chains about equilibrium positions to concerted motions of entire domains as the protein structure changes between equilibrium conformations. Both fluctuational dynamics and transitions between equilibrium conformations (either local or global) depend upon environmental factors. However, the various levels of protein dynamics may exhibit different responses to solvent viscosity. Motions at the protein surface or concerted motions of protein domains would be expected to be quite sensitive to solution properties, whereas local dynamics of the protein interior are influenced by viscosity only to the extent that they are coupled to more global dynamics. This study examines the extent to which protein–solvent interactions directly affect the ligand binding dynamics at the heme active site of hemoglobin.

The kinetics of ligand (CO, O_2) binding to hemoglobin (Hb) and myoglobin (Mb) have been well characterized by transient absorption measurements (Morris & Gibson, 1984; Gibson et al., 1986; Campbell et al., 1985; Hasinoff & Chishti, 1983, 1982; Hasinoff, 1981; Beece et al., 1980; Doster et al., 1982; Austin et al., 1975). In particular, Frauenfelder and co-workers have used this technique to great advantage. Their analyses of ligand rebinding subsequent to photolysis over a wide range of temperatures and solution conditions have revealed a power-law behavior for religation which can be described as motion of the ligand over a series of potential energy barriers each having a distribution of heights that is dependent upon the conformational properties of the protein. Several transient absorption studies have demonstrated the dependence of ligand recombination rates upon solvent viscosity (Hasinoff & Chishti, 1982, 1980; Hasinoff, 1981). A more detailed analysis of MbCO by Frauenfelder and co-workers (Beece et al., 1980) revealed that all except the innermost potential barriers encountered by the migrating ligand were viscosity dependent. This clearly implies that protein–solvent dynamics can regulate the dynamics of the interior protein motions.

The time-resolved resonance Raman techniques employed in this study provide data that complement the transient absorption studies. Resonance Raman scattering selectively interrogates the heme active site of hemoglobin. Moreover, the heme vibrational spectrum can be interpreted to provide specific molecular details about the active site (Spiro, 1983; Rousseau & Ondrias, 1983). Recently, time-resolved reso-

† This work was performed at the University of New Mexico and was supported by the NSF (DMB8604435).
‡ University of New Mexico.
§ AT&T Bell Laboratories.

0006-2960/88/0427-8719$01.50/0

nance Raman spectroscopy has been used to trace the structural evolution of the heme itself (on a picosecond to nanosecond time scale) and the relaxation of the heme pocket (on a nanosecond to millisecond time scale), subsequent to ligand photolysis, from a variety of hemoglobins (Rousseau & Friedman, 1988; Friedman et al., 1982a,b, 1983; Lyons et al., 1978; Stein et al., 1982; Friedman & Lyons, 1980; Terner et al., 1981; Dasgupta et al., 1985; Friedman, 1985; Scott & Friedman, 1984; Findsen et al., 1985a,b; Ondrias et al., 1983; Carson et al., 1987). These dynamics at the active site have been shown to depend upon allosteric effectors and the species of hemoglobin in question and have been directly correlated to the ligand binding properties of the proteins.

This work expands upon these previous studies and demosntrates that the dynamics of heme-pocket evolution in hemoglobin, subsequent to CO photolysis, are quite dependent upon solvent viscosity. They are thus most likely predicated upon large-scale protein motions that are communicated to the solvent.

Materials and Methods

HbA was purified from fresh whole cells following a modification of the procedure of Antonini and Brunori (1971), dialyzed against appropriate buffered solutions, concentrated to ~2 mM, and stored as HbCO. This stock HbCO was diluted to ~200 μM in mixtures of 50 mM Tris, inositol hexaphosphate (IHP), and glycerol (Aldrich Chemical Co.) so that the final solutions were at pH 6.5 ± 0.1, ~3 mM in IHP, or pH 8.9 ± 0.1 and contained ratios of glycerol to water accurate to ±2%. Those solutions were placed in anaerobic cuvettes, deoxygenated by several pump/purge cycles of N_2 gas followed by the addition of a slight amount of sodium dithionite, and placed under 1 atm of CO_2-free carbon monoxide. In view of the demonstrated sensitivity of heme-pocket relaxation rates to solution pH (Scott & Friedman, 1984), rigorous precautions were taken to ensure that all samples were prepared from the same stock solutions and adjusted to have identical pH and IHP concentrations. Sample pH was checked immediately before and immediately after experimental runs.

Time-resolved resonance Raman spectra were obtained via protocols described, in detail, elsewhere (Findsen, 1986; Findsen & Ondrias, 1988). An ~145° backscattering geometry was employed. Sample temperature was maintained at 20 ± 1 °C by direct flow of cooled N_2 gas onto the cuvette and continuously monitored via a platinum resistance probe placed on the cuvette window. Pulses of 532 nm from a frequency-doubled Nd:YAG laser (Spectra-Physics) were used to photolyze the sample. Resonance Raman spectra were obtained with 440-nm pulses from a nitrogen-pumped dye laser (Molectron) synchronized (to ±10 ns) with the photolysis laser. Cylindrical optics were used to focus both pulse trains on the sample. Power densities at the sample were controlled with neutral density filters. The power of the probe laser (440 nm) was reduced to the point where it produced minimal (<10%) photolysis of the ligated species. Peak positions were estimated by taking the midpoint of the full line width at half-maximum, yielding a precision of ±1 cm^{-1}.

Results

Photolysis of CO from hemoglobin results in a metastable heme-protein geometry that evolves toward the steady-state unligated conformation until it rebinds a ligand. Resonance Raman spectra of the heme active sites, obtained subsequent to photolysis of hemoglobin samples prepared in solutions of varying glycerol–water compositions, reveal the dependencies of both ligand rebinding and heme-pocket relaxation upon

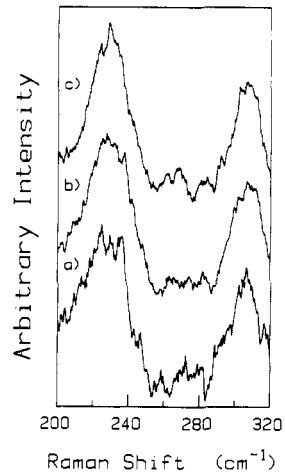

FIGURE 1: Resonance Raman spectra of photolyzed heme transient species at pH 6.5 + IHP obtained within 10 ns of CO photolysis. Samples were prepared as described in the text in solutions of (a) 25% ($\eta \approx 0.80$ cP), (b) 50% ($\eta \approx 1.7$ cP), and (c) 75% ($\eta \approx 3.50$ cP) glycerol, respectively. The temperature was maintained at 20 ± 1 °C. Spectra were obtained with ~440-nm laser pulses and a spectral band-pass of 7–8 cm^{-1}. They are the unsmoothed sums of three to five scans.

solvent viscosity. Resonance Raman spectra of samples with glycerol–water compositions of 0:100, 25:75, 50:50, and 75:25 by weight were obtained for (1) equilibrium HbCO, (2) the initial (10 ns) photolytic transient species, and (3) the photolyzed sites as they evolved in time over a 10-ns to 500-μs time range. Details of each set of experiments are given in the figure captions.

The effects of increasing levels of glycerol in the solvent mixture are quite benign with respect to the vibrational properties of either the equilibrium-ligated or initial (10 ns) photodissociated transient configurations of the heme. The resonance Raman spectra of HbCO in 75% glycerol, obtained with 406-nm excitation (not shown), were virtually identical with those of HbCO in buffered H_2O solution. Low-frequency spectra of the photolytic transient species, obtained with 10-ns pulses at 440 nm (see Figure 1), were found to be independent of the glycerol:water ratio of the solvent. They exhibited a pattern of shifts relative to that of equilibrium deoxy-Hb which is quantitatively consistent with the previously observed transient behavior of HbA in buffered solutions. The behavior of the Fe–proximal histidine stretching mode is of particular importance. Its position has been shown to be a sensitive indicator of the proximal heme-pocket configuration and relaxation dynamics (Scott & Friedman, 1984; Friedman, 1985; Friedman et al., 1982a,b; Stein et al., 1982; Findsen et al., 1985a). Its initial (10 ns) position in the spectra of photolytic transients is pH dependent (229 ± 1 cm^{-1} for pH 6.5 + IHP, 231 ± 1 cm^{-1} for pH 8.9) but is apparently independent of solvent composition.

While the initial configuration of the heme pocket in the Hb photolytic transients was invariant in the various glycerol–water samples, ligand rebinding kinetics and heme-pocket dynamics subsequent to photolysis were found to be quite sensitive to solvent viscosity. Figure 2 depicts the behavior of the heme ν_4 mode as a function of time and solvent composition for the pH 6.5 + IHP sample. The ratios of the deoxy (~1355 cm^{-1}) and ligated (~1374 cm^{-1}) forms of this mode can be used to assess the extent of ligand recombination following photolysis. The experimental conditions are such that the pump pulse photolyzes virtually all heme sites. The delayed probe pulse is attenuated to minimize its photolysis of rebound heme–CO sites. At all solvent compositions, a

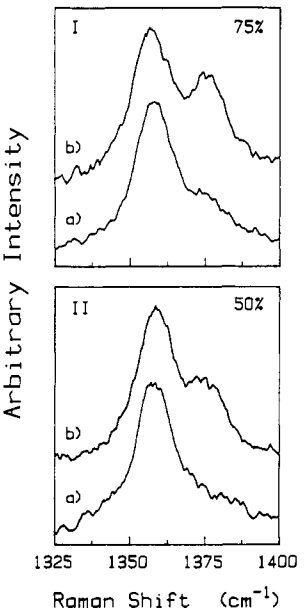

FIGURE 2: Time-evolution of ν_4 subsequent to complete CO photolysis from HbCO samples at pH 6.5 + IHP in (I) 75% glycerol and (II) 50% glycerol. Spectra were obtained via the two-pulse protocol described in the text at time delays of (a) 5 and (b) 500 μs. The probe pulses (440 nm) were attenuated to produce minimal photolysis of the rebound HbCO. Spectra are the unsmoothed sums of three to five scans at 7–8-cm^{-1} spectral band-pass.

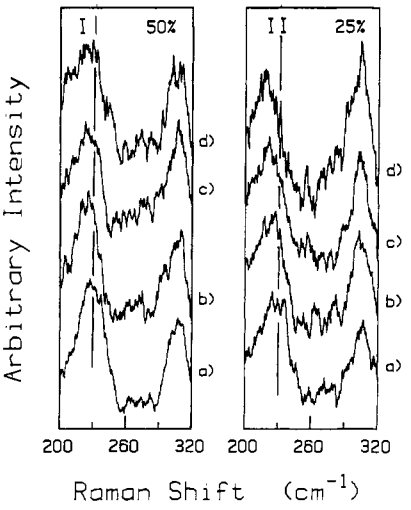

FIGURE 3: Time evolution of the ν_{Fe-His} mode (230–220 cm^{-1}) of the transient deoxyheme sites subsequent to CO photolysis at pH 6.5 + IHP: (I) 50% glycerol with Δt of (a) 10 ns, (b) 50 μs, (c) 500 μs, and (d) 1.7 ms; (II) 25% glycerol with Δt of (a) 10 ns, (b) 5 μs, (c) 50 μs, and (d) 150 μs. Conditions were the same as in Figure 2.

fraction of the photolyzed CO recombines on a submicrosecond time scale. This is undoubtedly geminate recombination of CO that does not escape from the distal heme pocket and is quantitatively consistent with the amount of geminate recombination observed in previous studies of HbA at pH <7.0 in the presence of IHP. At later times (>100 μs), additional CO rebinding is observed, the extent of which is governed by solvent composition. At higher glycerol concentrations, faster rebinding kinetics are observed.

The most obvious manifestation of solvent composition upon the dynamics of Hb photolytic transients is its effect upon heme-pocket relaxation kinetics. A series of low-frequency resonance Raman spectra obtained subsequent to CO photolysis in 25% and 50% glycerol samples maintained at 20 °C is shown in Figure 3. Solution conditions (pH 6.5, 3 mM IHP) were rigorously controlled and deliberately chosen to

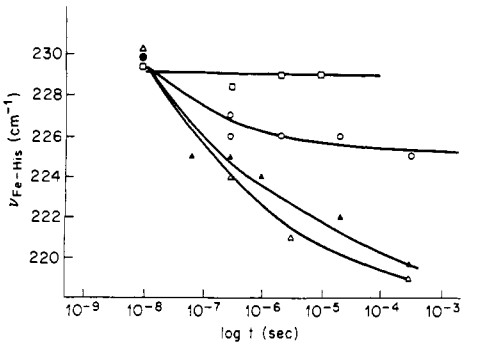

FIGURE 4: Plot of ν_{Fe-His} vs log t for photolyzed HbCO at pH 6.5 + IHP with varying glycerol content: (△) 0%, (▲) 25%, (○) 50%, and (□) 75% by weight. Precision of the data points is ±1 cm^{-1} and ±20 ns.

enhance the relaxation rate of the proximal pocket (Scott & Friedman, 1984). The evolution of the Fe–His mode toward its equilibrium deoxy position and relative intensity is clearly evident. The rate of ν_{Fe-His} (and by inference, proximal heme pocket) relaxation is strongly modulated by the glycerol–water composition of the solvent as shown in Figure 4. In 75% glycerol, little or no relaxation of ν_{Fe-His} occurs on a 10-ns to 1-ms time scale, while the relaxation kinetics in 25% glycerol are roughly equivalent to those observed in buffered water solution at pH 6.5 in the presence of IHP. The 50% glycerol samples exhibit relaxation at a slower rate. ν_{Fe-His} has relaxed only to 224 cm^{-1} after 1 ms (the longest time point of our experimental protocol). Thus, the half-life for relaxation in 50% glycerol is at least 2 orders of magnitude larger than those in buffered solution. Moreover, the heme-pocket relaxation rates of 25% and 50% glycerol samples were found to be quite sensitive to relatively small temperature variations (±5 °C). Although a comprehensive quantitative study was not conducted, it was clear that even a small decrease in temperature dramatically slowed heme-pocket relaxation.

Heme-pocket relaxation kinetics were also suppressed by increased glycerol concentration at pH 8.9. Under these conditions, the 0% and 25% glycerol samples again displayed similar relaxation rates which were consistent with previously reported observations (Scott & Friedman, 1984). Both yielded ν_{Fe-His} positions of 229 ± 1 cm^{-1} at 10 μs subsequent to CO photolysis. No relaxation of ν_{Fe-His} within the ±1-cm^{-1} precision of the measurements was evident on this time scale for the 50% glycerol sample.

The fact that ν_{Fe-His} relaxation kinetics are sensitive to factors that directly effect bulk viscosity (modest temperature reduction, increased glycerol concentration from 25% to 50%) while they are unaffected by glycerol concentrations up to ~3 M (25%) indicates that, if specific protein–glycerol binding interactions exist, they play no significant role in modulating heme-pocket dynamics. We conclude that variation of solvent viscosity is responsible for the observed effects.

Discussion

The dynamics associated with ligand binding in hemoglobin involve a number of phenomenologically distinct processes that are accessible to study by a variety of experimental and theoretical techniques. These include (1) the rapid (less than nanosecond) creation of a dissociated heme–CO pair producing a transient heme-pocket geometry, (2) the evolution of the heme-protein geometry to an equilibrium deoxy configuration, (3) movement of the ligand to and from the distal heme pocket, (4) the ligand migration through the protein matrix to and from the solvent interface, (5) the diffusion of the ligand to

and from the solution, and (6) the ultimate rebinding of the ligand to the transient or equilibrium deoxyheme.

Ligand rebinding kinetics subsequent to photolysis have been extensively analyzed in terms of the activation barriers associated with ligand movement from solvent to active site. Conformational dynamics have been postulated to play a role in the observed heterogeneity in these barriers (Beece et al., 1980; Doster et al., 1982; Austin et al., 1975). The heme active site undergoes large conformational changes upon ligand binding (Perutz, 1970; Baldwin & Chothia, 1979; Fermi et al., 1984). These are almost surely communicated to the rest of the protein by large-scale concerted motions, triggered at the heme, that ultimately result in quaternary and tertiary conformational changes between equilibrium deoxy and ligated forms of the system. Transient absorption (Hofrichter et al., 1983; Martin et al., 1983; Friedman et al., 1985), resonance Raman [see Rousseau and Friedman (1985) for review], and molecular dynamics calculations (Henry et al., 1985) of ligand photolysis in hemoglobins and myoglobins strongly suggest that the heme-pocket structural dynamics, immediately ($\leq$10 ns) subsequent to ligand photolysis, involve the elastic response of the heme and protein residues in direct contact with it. Subsequently, the overall heme-pocket geometry relaxes to its equilibrium configuration on a nanosecond to millisecond time scale. The kinetics of this process are dependent upon both protein and environmental conditions (Friedman et al., 1982a,b, 1985; Lyons & Friedman, 1980; Scott & Friedman, 1984; Ondrias et al., 1983, Findsen et al., 1986).

The time-resolved resonance Raman data presented above directly or indirectly probe processes 1, 2, 3, and 6 and provide experimental evidence that the structural relaxation of the proximal heme pocket, subsequent to ligand photolysis, is communicated to the solvent.

Initial Transient Heme-Pocket Geometry. The spectra in Figure 1 demonstrate that the initial ($\leq$10 ns) heme-pocket geometry established subsequent to the relaxation of the heme to its deoxy configuration is not dependent upon solvent viscosity. These findings confirm the notion that initial heme-pocket dynamics following photolysis are local in nature constituting an elastic response to the heme structural changes. Theoretical studies by Karplus and co-workers (Gelin & Karplus, 1977; Gelin et al., 1983) indicate that two types of perturbations characterize the initial heme-pocket dynamcs: heme translation and heme tilting. Heme translation results from the doming of the heme as the iron atom moves out of plane. Subsequent tilting of the heme occurs without significant change in the position of the F–G corner. The increased frequency of ν_{Fe-His} in the transient species relative to that in the equilibrium species has been postulated to arise from more upright posture of the proximal histidine (in its own plane) relative to the heme (Friedman et al., 1982a,b; Friedman, 1985). This geometry minimizes steric repulsion between the heme pyrrole nitrogens and histidine β-carbon, thus strengthening the Fe–His bond. Apparently, these local rearrangements occur without significant changes in the positions of the protein helices (in particular the F-helix).

The helix positions in equilibrium, ligated protein may, of course, still be influenced by environmental factors. The systematic variations of the Fe–His mode frequency with species, pH, and allosteric effectors in 10-ns photolytic transients (Friedman et al., 1983; Scott & Friedman, 1984; Friedman, 1985; Carson et al., 1987) must arise from these equilibrium constraints imposed upon the ligated globin conformations (and hence upon the initial heme-pocket geometry subsequent to photolysis).

Ligand Rebinding Kinetics. The rebinding of photolyzed CO to the heme has been shown to be a complex process in hemoglobins and myoglobins involving geminate ligand–heme recombination, ligand migration through the protein matrix, and ligand movement between the solvent and the protein matrix. A number of absorption studies have demonstrated that the bimolecular rates of heme–ligand binding are dependent upon solvent viscosity in very predictable ways (Hasinoff & Chishti, 1982, 1983). On the other hand, Frauenfelder and co-workers (Beece et al., 1980) have found that, in Mb, the innermost activation barrier is independent of solvent viscosity. Ligand migration through the protein matrix must involve motions of the side-chain residues which might be coupled to the solvent to varying degrees.

Our data (Figure 2) are qualitatively consistent with the above scenario. Direct quantification of the amount of ligand rebinding is difficult owing to the different resonance cross-sections for deoxyheme and ligated-heme sites. However, it is apparent that the extent of ligand rebinding (indicated by the relative intensity of the $\sim$1375-cm^{-1} band) is more solvent dependent at relatively long times ($\geq$100 μs).

The extent of geminate recombination subsequent to photolysis in hemoglobins has been shown to be quite sensitive to both heme-pocket tertiary structure and temperature (Scott & Friedman, 1984). To first order, it is predicated upon the relative barrier heights for ligand rebinding versus ligand escape from the distal pocket. Those barriers are modulated by the geometries and dynamics of the proximal and distal pockets, respectively.

Moreover, the rate of ligand escape from a potential well should be dependent upon the coupling between the well and its environment. This coupling is, in turn, dependent upon the viscosity of the medium. In the large coupling limit, the rate of escape will be proportional to η^{-1} [see Beece et al. (1980) for discussion]. Our data indicate that neither the proximal pocket geometry immediately after photolysis nor the barrier to ligand escape from the distal pocket displays a marked sensitivity to solvent viscosity. This clearly suggests that the barrier to ligand escape arises primarily from local motions of the protein interior which are relatively unaffected by solvent viscosity. Ligands that escape further into the protein matrix encounter solvent-dependent barriers that inhibit their diffusion through the protein matrix at higher solvent viscosities.

Our results are consistent with recent theoretical studies [Brooks et al. (1988) and references cited therein] which indicate that fluctuational dynamics are most pronounced at the protein surface. At higher solvent viscosities, fluctuations at the protein–solvent interface are significantly damped, thus inhibiting ligand movement between matrix and solvent. The net effect is to lower the probability of ligand escape into the solvent subsequent to photolysis, increasing the extent of ligand–heme recombination in the 100-μs to 1-ms time range.

Relaxation of the Proximal Heme Pocket. The evolution of the proximal heme pocket to its equilibrium deoxy conformation following ligand photolysis evidently results from protein dynamics of a different hierarchical nature than the local fluctuations that modulate the escape of the ligand from the distal heme pocket. These relaxation kinetics can be inferred from the temporal evolution of the position of ν_{Fe-His} subsequent to photolysis. Previous spectroscopic studies have established that the transient heme-pocket conformations generated by ligand photolysis relax to equilibrium deoxy configurations with rates that are pH and protein specific [see Rousseau and Friedman (1988)]. It remained uncertain, however, whether the variable relaxation dynamics and the

forces producing them were confined to the heme pocket or were reflective of conformational dynamics of larger protein domains. The effects of increasing glycerol concentration upon ν_{Fe-His} relaxation kinetics are completely consistent with solvent viscosity, playing a dominant role in proximal heme-pocket dynamics when other solution variables (pH, IHP concentration) are rigorously controlled.

Several aspects of the proximal heme-pocket dynamics suggest that they involve concerted motions of a large protein domain rather than localized dynamics. The time scale involved in heme-pocket relaxation (1–100 μs, depending upon environmental factors) is inconsistent with the isolated motions of individual side chains which are expected to be quite rapid at room temperature ($\leq$10 ns). Moreover, the pronounced change of heme-pocket relaxation kinetics for pH 6.5 + IHP samples over a rather modest range of solvent viscosity ($\eta \approx$ 0.80 cP to $\eta \approx$ 3.5 cP for 25% vs 75% glycerol solutions at 20 °C)[1] cannot be modeled by simple Stokes–Einstein "diffusional" motion of side chains.

The relative motion of α-helices has been postulated to play a functional role in a variety of nonheme enzymes (Lesk & Chothia, 1984; Chothia & Lesk, 1985). Crystallographic and theoretical studies suggest a likely role for similar motions in hemoglobin. The X-ray diffraction data of Perutz (1970) and others (Baldwin & Chothia, 1979; Fermi et al., 1984; Anderson, 1975) indicate that the largest structural changes between the equilibrium R and T states of hemoglobin occur at the $\alpha_1\beta_2$ interface region, within the heme pocket, and along segments of the F-helix and F–G corner. In particular, the F–G corners of the $\alpha_1\beta_1$ and $\alpha_2\beta_2$ dimers are moved 2.5 Å further apart, while the F-helix itself moves $\sim$1.5 Å relative to the heme (Baldwin & Chothia, 1979). Karplus and coworkers (Gelin & Karplus, 1977; Gelin et al., 1983) have suggested that these regions comprise an "allosteric core" of the protein and theoretically modeled its structural and dynamic characteristics. They concluded that this region most likely serves as the vehicle for the communication of cooperative energetics between heme sites.

The F-helix and F–G corner comprise a major portion of the proximal heme pocket and are significantly exposed to solvent (Perutz, 1970; Baldwin & Chothia, 1979; Fermi et al., 1984). Thus, the motions of this region associated with conformational changes should be both sensitive to solvent viscosity and pivotal to proximal heme-pocket dynamics. The fact that initial heme-pocket geometry, subsequent to photolysis, is insensitive to solvent viscosity, but that heme-pocket relaxation kinetics are quite viscosity dependent, supports models of protein dynamics that include large-scale motions of the F-helix as the basis for proximal heme-pocket relaxation. These motions are probably directly responsible for the propagation of structural changes and for ligand binding cooperativity between the heme active sites and the subunit interface.

Conclusions

The influence of solvent viscosity upon the various dynamic processes initiated by CO photolysis from the heme active site of hemoglobin can be used to distinguish whether those processes are local or global in nature. The resonance Raman data obtained in this study yield the following insights into the ligand binding dynamics of hemoglobin: (1) The species-specific proximal heme-pocket geometry of the photolytic transient species generated within 10 ns of CO photolysis is independent of solvent viscosity, but quite sensitive to pH and allosteric effectors. This clearly indicates that the initial evolution of the heme pocket is elastic and local in nature, with the 10-ns transient geometry determined by the solution-sensitive disposition of the equilibrium-ligated protein conformation. (2) Prompt ($\leq$1 μs) ligand–heme rebinding does not appear to be significantly influenced by solvent viscosity, while longer time rebinding is quite viscosity dependent. Apparently, the protein dynamics dictating the escape of the ligand from the distal pocket are local fluctuations that are insulated from the solvent, while the dynamics which modulate the ligand migration through the protein and across the protein–solvent interface are coupled to the solvent. (3) Subsequent relaxation of the metastable transient geometry is viscosity dependent, suggesting that it is predicated upon large-scale motions of the F-helix and, presumably, the entire "allosteric core" of the protein.

[1] Values obtained from *CRC Handbook of Chemical Engineering* (1984).

Acknowledgments

We thank Cecilia Wells for technical assistance in the purification and preparation of hemoglobin samples and acknowledge Prof. B. M. Pettit for helpful and stimulating discussions.

Registry No. HbA, 9034-51-9; CO, 630-08-0.

References

Anderson, L. (1975) *J. Mol. Biol. 94*, 33–49.

Antonini, E., & Brunori, M. (1971) *Hemoglobin and Myoglobin in Their Reaction with Ligands*, North-Holland, Amsterdam.

Austin, R. H., Beeson, K. W., Eisenstein, L., Frauenfelder, H., & Gunsalus, I. C. (1975) *Biochemistry 14*, 5355–5373.

Baldwin, J., & Chothia, C. (1979) *J. Mol. Biol. 129*, 175–220.

Beece, D. Eisenstein, H., Frauenfelder, H., Good, D., Marden, M. C., Reinisch, A., Reynolds, A. H., Sorensen, L. B., & Yue, K. T. (1980) *Biochemistry 19*, 5147–5157.

Brooks, C. L., Karplus, M., & Pettit, B. M. (1988) *Adv. Chem. Phys.* (in press).

Campbell, B. F., Magde, D., & Sharma, V. (1985) *J. Biol. Chem. 260*, 2752–2756.

Carson, S. D., Wells, C. A., Findsen, E. W., Friedman, J. M., & Ondrias, M. R. (1987) *J. Biol. Chem. 262*, 3044.

Chothia, C., & Lesk, A. M. (1985) *Trends Biochem. Sci. (Pers. Ed.) 10*, 116–118.

CRC Handbook of Chemical Engineering (1984) CRC, Boca Raton, FL.

Dasgupta, T., Spiro, T. G., Johnson, C. K., Dalickas, G. A., & Hochstrasser, R. M. (1985) *Biochemistry 24*, 5295–5297.

Debrunner, P. G., & Frauenfelder, H. (1982) *Annu. Rev. Phys. Chem. 33*, 283.

Doster, W., Beece, D., Browne, S. F., DiIorio, E. E., Eisenstein, L., Frauenfelder, H. Reinisch, L., Shyamsunder, E., Winterhalter, K. H., & Yue, K. T. (1982) *Biochemistry 21*, 4831–4839.

Fermi, G. Perutz, M. F., Shaanan, B., & Fourme, R. (1984) *J. Mol. Biol. 175*, 159–174.

Findsen, E. W. (1986) Ph.D. Dissertation, University of New Mexico.

Findsen, E. W., & Ondrias, M. R. (1988) *Appl. Spectrosc. 42*, 445–450.

Findsen, E. W., Friedman, J. M., Ondrias, M. R., & Simon, S. R. (1985a) *Science (Washington, D.C.) 229*, 661–665.

Findsen, E. W., Scott, T. W., Chance, M. R., Friedman, J. M., & Ondrias, M. R. (1985b) *J. Am. Chem. Soc. 107*, 3355–3357.

Findsen, E. W., Simons, P., & Ondrias, M. R. (1986) *Biochemistry 25*, 7912.
Friedman, J. M. (1985) *Science (Washington, D.C.) 228*, 1273-1280.
Friedman, J. M., & Lyons, K. B. (1980) *Nature (London) 284*, 570-579.
Friedman, J. M., Rousseau, D. L., Ondrias, M. R., & Stepnoski, R. A. (1982a) *Science (Washington, D.C.) 218*, 1244-1246.
Friedman, J. M., Ondrias, M. R., & Rousseau, D. L. (1982b) *Annu. Rev. Phys. Chem. 33*, 471.
Friedman, J. M., Scott, T. W., Stepnoski, R. A., Ikeda-Saito, M., & Yonetani, J. (1983) *J. Biol. Chem. 258*, 10564-10573.
Friedman, J. M., Scott, T. W., Fisanick, G. J., Simon, S. R., Findsen, E. W., Ondrias, M. R., & MacDonald, V. R. (1985) *Science (Washington, D.C.) 229*, 187.
Gelin, B. R., & Karplus, M. (1977) *Proc. Natl. Acad. Sci. U.S.A. 74*, 801-805.
Gelin, B. R., Lee, A. W.-M., & Karplus, M. (1983) *J. Mol. Biol. 171*, 489-559.
Gibson, Q. H., Olson, J. S., McKinnie, R. E., & Rohlfs, G. (1986) *J. Biol. Chem. 261*, 10228-10229.
Gurd, F. R. N., & Rothgeb, T. J. (1979) *Adv. Protein Chem. 33*, 74.
Hartman, H., Park, F., Steigeman, W., Petsko, G. A., Ponzi, D. R., & Frauenfelder, H. (1982) *Proc. Natl. Acad. Sci. U.S.A. 79*, 4967.
Hasinoff, B. B. (1981) *J. Phys. Chem. 85*, 528-531.
Hasinoff, B. B., & Chishti, S. B. (1982) *Biochemistry 21*, 4275-4278.
Hasinoff, B. B., & Chishti, S. B. (1983) *Biochemistry 22*, 58-61.
Henry, E. R., Levitt, M., & Eaton, W. A. (1985) *Proc. Natl. Acad. Sci. U.S.A. 82*, 2034-2038.
Hofrichter, J., Sommer, J. H., Henry, E. R., & Eaton, W. A. (1983) *Proc. Natl. Acad. Sci. U.S.A. 80*, 2235.
Karplus, M., & McCammon, A. (1983) *Annu. Rev. Biochem. 53*, 263-300.
Lesk, A. M., & Chothia, C. (1984) *J. Mol. Biol. 174*, 175-191.
Lyons, K. B., Friedman, J. M., & Fleury, P. A. (1978) *Nature (London) 275*, 565-566.
Martin, J. L., Nigus, A., Poyant, C., Lecarpentier, Y., Astier, R., & Antonetti, A. (1983) *Proc. Natl. Acad. Sci. U.S.A. 80*, 173.
Morris, R. J., & Gibson, Q. H. (1984) *J. Biol. Chem 259*, 367-374.
Ondrias, M. R., Friedman, J. M., & Rousseau, D. L. (1983) *Science (Washington, D.C.) 220*, 615-619.
Perutz, M. F. (1970) *Nature (London) 228*, 726-734.
Rousseau, D. L., & Ondrias, M. R. (1983) *Annu. Rev. Biophys. Bioeng. 12*, 357-380.
Rousseau, D. L., & Friedman, J. M. (1988) in *Biological Application of Raman Scattering* (Spiro, T. G., Ed.) Vol. III, Wiley, New York.
Scott, T. W., & Friedman, J. M. (1984) *J. Am. Chem. Soc. 106*, 5677-5687.
Spiro, T. G. (1983) in *Iron Porphyrins* (Lever, A. B. P., & Gray, H. B., Eds.) Vol. II, pp 89-139, Addison-Wesley, Reading, MA.
Stein, P., Terner, J., & Spiro, T. G. (1982) *J. Phys. Chem. 86*, 168-172.
Terner, J., Stong, J. D., Spiro, T. G., Nagumo, M., Nicol, M. S., & El-Sayed, M. A. (1981) *Proc. Natl. Acad. Sci. U.S.A. 78*, 1313-1317.

Spontaneous Vesiculation of Large Multilamellar Vesicles Composed of Saturated Phosphatidylcholine and Phosphatidylglycerol Mixtures†

T. D. Madden,*,‡ C. P. S. Tilcock, K. Wong, and P. R. Cullis‡
Department of Biochemistry, The University of British Columbia, Vancouver, British Columbia V6T 1W5, Canada
Received May 3, 1988; Revised Manuscript Received July 11, 1988

ABSTRACT: The influence of temperature and ionic strength on the vesiculation properties of large multilamellar vesicles containing various proportions of dimyristoylphosphatidylglycerol has been investigated. It is shown that at low ionic strengths preformed large multilamellar vesicles composed of dimyristoylphosphatidylcholine and dimyristoylphosphatidylglycerol (7:3) on incubation at the gel to liquid-crystalline transition temperature (T_c ~23 °C) spontaneously vesiculate to form predominantly unilamellar systems with a mean diameter of 120 nm. Such vesiculation is not observed for incubations at temperatures appreciably above or below T_c, and is also inhibited by higher ionic strengths. Stable large multilamellar vesicles are formed, however, in systems containing the dioleoyl species of phosphatidylcholine or phosphatidylglycerol and also for dimyristoylphosphatidylcholine/dimyristoylphosphatidylserine mixtures. The vesiculation properties of dimyristoylphosphatidylcholine/dimyristoylphosphatidylglycerol mixtures, therefore, appear to reflect an instability in the region of the T_c driven by surface potential effects which are specific for the glycerol headgroup.

Upon hydration, most naturally occurring phospholipids adopt either the bilayer organization or the hexagonal H_{II} phase (Cullis & de Kruijff, 1979; Cullis et al., 1985). In both instances, the macromolecular structures formed are large (several micrometers) and stable such that even transitions between these polymorphic phases do not generate small vesicles. One exception is the case of cardiolipin which in the presence of calcium adopts the hexagonal H_{II} phase. If this mixture is dialyzed against EDTA, small vesicles are generated

† This research was supported by the Medical Research Council of Canada and The Liposome Co., Princeton, NJ.
‡ Present address: The Canadian Liposome Co., Ltd., Suite 308, 267 West Esplanade, North Vancouver, British Columbia V7M 1A5, Canada.

0006-2960/88/0427-8724$01.50/0